ASEAN Journal of Chemical Engineering 2023, Vol. 23, No. 3, 329 – 342

Photocatalytic Degradation Activity of the Biosynthesized *R. rosifolius* Mediated Silver Nanoparticles in Methylene Blue Dye

Marilen M. Martin [1,2]
Rodolfo E. Sumayao, Jr. [2]
Allan N. Soriano [*,3]
Rugi Vicente C. Rubi [4]

[1] *School of Chemical, Biological, and Materials Engineering and Sciences, Mapúa University, 658 Muralla St. Intramuros, Manila, Philippines*
[2] *Department of Chemistry, William Shaw College of Science, De La Salle University, 2401 Taft Avenue, Manila, Philippines*
[3] *Department of Chemical Engineering, Gokongwei College of Engineering, De La Salle University, 2401 Taft Avenue, Manila, Philippines*
[4] *Chemical Engineering Department, College of Engineering, Adamson University, 900 San Marcelino St. Ermita, Manila, Philippines*
[*]*e-mail:* allan.soriano@dlsu.edu.ph

Submitted 22 February 2023 *Revised* 20 July 2023 *Accepted* 4 August 2023

Abstract. Water pollution is a chronic problem affecting the entire ecosystem. To partly remediate water pollution, wastewater treatment prior to disposal must be done regularly. Here, the photocatalytic degradation of methylene blue (MB) dye was assessed using *R. rosifolius Linn* (also known as sampinit) aqueous fruit extract silver nanoparticles (SAFE-AgNPs). In this study, the SAFE-AgNPs were utilized to remediate wastewater contaminated with methylene blue (MB) dye which is harmful to the environment, aquatic and human lives. As previously described, SAFE-AgNPs were synthesized via a simple 'one-pot' approach. SAFE-AgNPs were assessed for their photocatalytic reduction of MB dye following sunlight or LED irradiation. Kinetic adsorption models were employed to determine the adsorption uptake of MB by SAFE-AgNPs. Photocatalytic degradation of methylene blue by SAFE-AgNPs was achieved under sunlight and LED irradiations at 98.8% and 97.6%, respectively. These results on the photocatalytic degradation of MB by SAFE-AgNPs may offer a potential strategy in wastewater treatment.

Keywords: Methylene Blue Dye, Photocatalytic Degradation, Silver Nanoparticles, Wastewater Treatment

INTRODUCTION

Water pollution is a global concern threatening the whole ecosystem. According to the water environment partnership in Asia (WEPA), there are about 85,000 manufacturing industries in the Philippines, with Metro Manila as the prime industrial region (WEPA, 2015). The quality of Philippine waters has been reduced due to rapid population, urbanization, and industrialization, especially in densely populated areas and regions of industrial and agricultural activities (WEPA, 2015). Access to

DOI: 10.22146/ajche.82506

clean and adequate water remains a problem in urban and coastal regions in the Philippines. The significant liquid waste discharge disposed to water sources as effluents include dyes, heavy metals, and dissolved organic contaminants (Fahimirad *et al.*, 2017; Hatami *et al.*, 2017). Contamination of the water bodies by these effluents poses a significant threat to all living things and the biogeochemical cycles due to high resistance to degradation of these pollutants (Kharissova *et al.*, 2013). MB dye is the industrial organic dye waste to consider in this study. The presence of this dye in water would be very detrimental to the aquatic environment and human health. Scientists are now faced with a very challenging task to provide efficient methods for dye degradation. Several conventional techniques are available to remove dye wastes, such as ultraviolet light (UV) degradation and sorption protocol (Abbasi *et al.*, 2016). But due to the high cost and less efficiency of these techniques, there is a need to search for more advanced methods to handle these hazardous pollutants. Green chemistry is imperative to help remediate water pollution. The biological process through plant extract is of utmost consideration in this study since it does not use hazardous chemicals, is simple, and is inexpensive. So, an imminent need to develop a novel technique for removing dye waste that is more efficient is of prime importance to research.

The silver nanoparticles used were synthesized from the aqueous fruit extract of *R. rosifolius*, also known as Sampinit, from the previous study (Martin and Sumayao Jr., 2022). It is named Sampinit aqueous fruit extract silver nanoparticles or SAFE-AgNPs. The biosynthesized SAFE-AgNPs previously prepared produced desirable optical, biophysical, and structural properties, which are good characteristics of potent photocatalysts to remediate wastewater (Martin and Sumayao Jr., 2022). As such, it was used in this study's photodegradation of MB dye.

The present study aimed to investigate the catalytic potential of *R. rosifolius*-based biogenic AgNPs by the photocatalytic degradation of MB dye solution under sunlight and LED light irradiations. The kinetic properties of SAFE-AgNPs on the degradation of MB dye using mathematical adsorption kinetic models, namely, Lagergen's pseudo first order (PFO), Ho's pseudo second order (PSO), Elovich, and Intraparticle diffusion (IPD) models, were determined. To further establish the catalytic behavior of SAFE-AgNPs, Langmuir Hinshelwood (L-H) model was applied to the system. The resulting L-H data complemented the results provided by one of the chemical adsorption kinetic models employed in the study.

This research can help one better understand the general mechanism governing the adsorption process on the degradation of MB dye by SAFE-AgNPs. In engineering practice, this will offer a clearer picture in designing an industrial degradation reactor to provide the solution to wastewater treatment.

EXPERIMENTAL SECTION

Chemicals

All other materials were obtained from Merck (previously known as Sigma-Aldrich) in Germany unless otherwise stated.

SAFE-AgNPs

The biosynthesized AgNPs used in this study were prepared and characterized from the

previous report (Martin and Sumayao Jr., 2022).

Photocatalytic Reduction of MB Dye by SAFE-AgNPs

For the photocatalytic reduction of MB dye, 40.00 mL of 0.10 M $NaBH_4$ was added to 20.00 ml of 100.00 ppm MB solution. Then, 5.00 mL of 0.88 mg/mL SAFE-AgNPs was added to the mixture and diluted with 20.00 mL DDI water. It was constantly stirred at room temperature (25°C ± 2°C) and was carried out in a customized photocatalytic reactor equipped with an LED lamp (with 40W; 220V power) and aided with a cooling fan. See Figure 1. A 3.0 ml aliquot of the samples was collected periodically every 60 minutes and centrifuged at 12,000 rpm for 20 minutes. It was compared with the catalytic performance of the synthetic AgNPs with 20 ppm concentration. Before the photocatalytic experiment, the solution was magnetically stirred for 30 minutes in the dark to establish the adsorption-desorption equilibrium between the dye and the catalyst. The photocatalytic degradation of MB was monitored by measuring its absorbance from the 200-800 nm range using a UV-Vis spectrophotometer (Hitachi U-2900, Tokyo, Japan) at regular time intervals. The same procedure exposed MB solution to direct sunlight from 11:00 AM – 3:00 PM. A control containing only MB solution with $NaBH_4$ was prepared and subjected to the same experimental procedures cited above. The Equation (1) computed the percent dye degradation.

$$\%\ dye\ degradation = \frac{MBo - MB}{MB_o} x100 \qquad (1)$$

MB_o is the initial absorption intensity at λmax = 663 nm, and M_B is the absorption intensity after photocatalytic dye degradation.

Recyclability of SAFE-AgNPs

Upon MB dye degradation, the photodegraded sample was centrifuged at RT for 20 minutes to collect the SAFE-AgNPs used in the solution. The collected precipitate was washed twice with DDI water, oven dried at 50°C, and weighed. It was reused for the next cycle under the same conditions.

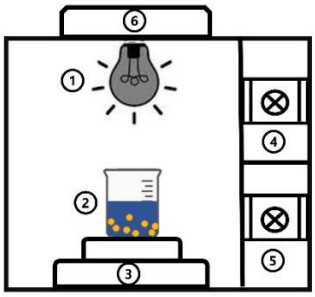

Fig 1: Schematic diagram of fabricated photocatalytic reactor, (1) LED bulb, (2) methylene blue sample + SAFE-AgNPs, (3) mixing plate, (4) mixing controller, (5) temperature controller, and (6) exhaust fan.

RESULTS AND DISCUSSION

Photocatalytic Properties of SAFE-AgNPs

The photocatalysis of the biosynthesized SAFE-AgNPs to stimulate MB dye degradation was explored. The reaction mixture's absorbance was monitored over a 60-minute time interval. Dye degradation was associated with a change in color from deep blue to colorless solution (Chen *et al.*, 2007; Singh and Daliwal, 2020). Methylene blue is reduced to leucomethylene, as evidenced by the change in color (Edison and Sethuraman, 2012). The peak intensity of MB at 663 nm slowly decreased as the time of exposure to light sources, both LED and sunlight, increased, indicating successful photodegradation of the pollutant dye (Figure 2A). Figure 2B showed that MB degraded faster at 180 minutes in the

DOI: 10.22146/ajche.82506

presence of SAFE-AgNPs than the synthetic AgNPs, which fully degraded after 360 minutes under LED irradiation. Similarly, MB degraded faster at 100 minutes in the presence of SAFE-AgNPs than the synthetic AgNPs, which completely degraded after 180 minutes under sunlight irradiation (Figure 2C). 98.8% of MB was degraded over 100-minute exposure to sunlight, and around 97.6% of MB was degraded at 180 minutes under LED irradiation. Both use the as-synthesized SAFE-AgNPs as catalysts. These results showed that SAFE-AgNPs were an effective catalyst in the photodegradation of MB. Moreover, photodegradation of MB using SAFE-AgNPs under sunlight or LED irradiation is more favorable than the synthetic AgNPs. Indeed, sunlight is superior in activating metallic NPs as catalysts than other light sources (Mechouche *et al.*, 2022). These observations could be attributed to the numerous surface hydroxyl groups coating the SAFE-AgNPs that trap photoexcited electrons and holes, preventing electron hole pair recombination and resulting in an enhanced photodegradation process (Kumar *et al.*, 2019; Rostami-Vartooni, *et al.*, 2016). The faster degradation rate of MB with SAFE-AgNPs under sunlight exposure compared to LED light irradiation, Figures 3A and 3B, could be explained by the high temperature emitted by sunlight causing high energy electrons to be produced, generating oxygen free radicals ($O_2^{\bullet-}$). These free radicals interact with the environment of oxygen molecules and hydroxyl ions to form hydroxyl radicals (OH•). These radicals are the ones responsible for the degradation of these dye molecules. These results evidenced the catalytic efficiency of the as-synthesized SAFE-AgNPs to eliminate dye pollution. A study on the photodegradation of chlordane in water and soil showed the opposite findings on the influence of the induced UV light and sunlight on the photodegradation of the pesticide. Results exhibited a higher degradation rate of 91.65% in water and 62.54% in soil, both using UV light, whereasonly 71.59% in aqueous solution and 56.35% in soil, both under sunlight irradiation. These findings could be attributed to the nature of the samples, particulate matter that may contribute to light scattering, and the organic compounds acting as fillers (Sioson and Gallardo, 2008).

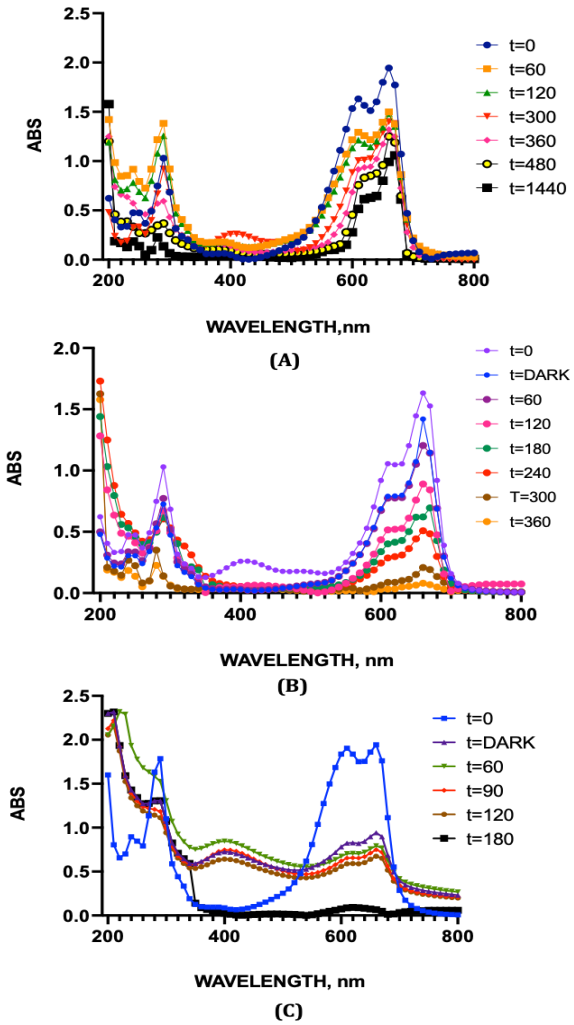

Fig. 2: UV-Vis absorption spectra of MB in the presence of different catalysts at different times under LED light irradiation. a) MB control; b) MB with synthetic AgNPs; c) MB with SAFE-AgNPs.

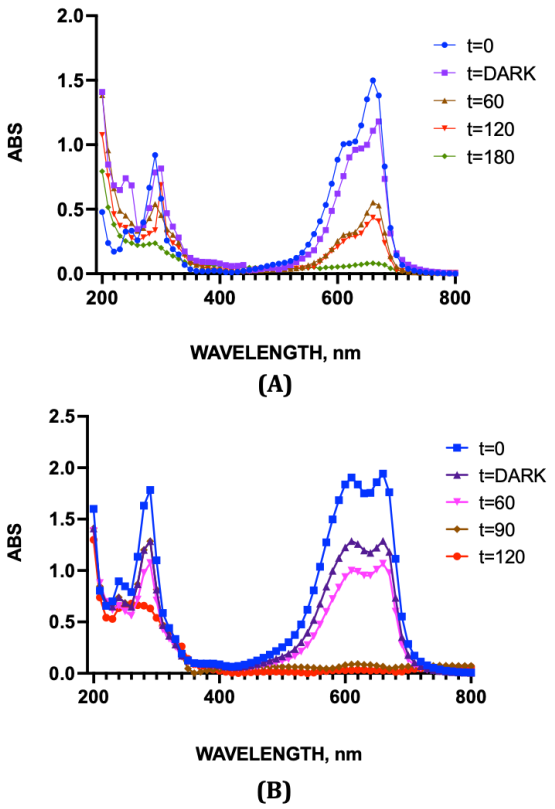

Fig. 3: UV-Vis adsorption spectra of MB in the presence of catalysts at different times under SUNLIGHT irradiation. A) MB with AgNPs; B) MB with SAFE-AgNPs

Meanwhile, MB control did not degrade completely even after longer exposure to either light source. MB dye reduction with $NaBH_4$ without the NP catalyst may be favorable and feasible thermodynamically but not so kinetically (Varadavenkatesan *et al.*, 2016). This is where the involvement of nanoparticles begins. It decreases the reaction's activation energy barrier, leading to a rapid and efficacious reduction process (Gupta *et al.*, 2011). Similar findings were discussed where MB dye was subjected to photodegradation without the presence of the biosynthesized AgNPs. Negligible MB dye decolorization and very low photocatalytic rate were observed (Ji *et al.*, 2018; Ajay *et al.*, 2022). Whereas some studies reported no appreciable decrease in the MB concentration was observed in the absence of the biosynthesized AgNPs prepared (Singh *et al.*, 2020; Mehwish *et al.*, 2021).

Rate of Reaction (Chemical Kinetics)

Four different mathematical adsorption kinetic models were employed in this study to measure the adsorption uptake of MB by SAFE-AgNPs concerning time at a constant concentration. This is used to measure the diffusion of the MB dye (adsorbate) to the biogenic SAFE-AgNPs (Saha and Grappe, 2017). It is important to note that the study of the adsorption kinetics is crucial in designing the adsorption process as it facilitates understanding the degradation mechanism of MB dye by SAFE-AgNPs.

The adsorption kinetics of the MB dye by the biogenic AgNPs is depicted mathematically by fitting experimental values to pseudo-first-order, pseudo-second order, Elovich, and intraparticular diffusion reactions (Ruíz-Baltazar, 2020 and Gowda *et al.*, 2022). This step is imperative in understanding the adsorption processes' underlying degradation mechanism, such as chemical reactions and mass transfer (Banerjee, 2012).

A. Lagergen's Pseudo first order (PFO) model (Aurich *et al.*, 2017) is given by the Equation (2).

$$ln\ (q_e - q_t) = ln\ q_e - k_1 t \qquad (2)$$

k_1 is the rate constant of the first-order adsorption expressed in min^{-1}, q_e the amount of MB polluted at equilibrium (mg/g), and qt is the amount of MB degraded by the AgNPs at any time, *t*, (mg/g). This model represents a typical adsorption kinetic analysis for the adsorption process.

DOI: 10.22146/ajche.82506

B. Ho's Pseudo second order (PSO) model (Ho, 2006) is given by Equation (3).

$$H_2=k_2\, q_e^2 \quad (3)$$

H_2 is the initial adsorption rate (mg/g min) as q_t/t approaches 0. The parameter H_2 will be calculated in the PSO models. This model provides information on the description and the evaluation of adsorption kinetics in diverse adsorption systems (Ho and McKay, 2000, Venkateswarlu *et al.*, 2007).

C. Elovich model (86) describes the adsorption process as chemisorption (Gowda *et al.*, 2022) and is represented by Equation (4).

$$q_t = \frac{1}{\beta}\ln(\alpha\beta) + \frac{1}{\beta} lnt \quad (4)$$

where α is the initial adsorption rate (mg·g^{-1}·min) and β desorption constant (g·mg^{-1}).

D. Intraparticle diffusion (IPD) model is necessary for determining the rate limiting step in the adsorption process and is described by Equation (5). (Gowda *et al.*, 2022)

$$q_t = k_i\sqrt{t} + C_i \quad (5)$$

where k_i is the rate constant of intraparticle diffusion expressed in (mg·g^{-1}·min$^{-0.5}$) and C_i is the intercept in the plot q_t versus $t^{1/2}$.

The PFO, PSO, Elovich, Intraparticle diffusion and L-H models, are reflected in Figures 4-8, respectively. The correlation factors are shown per model and catalyst to determine the theoretical kinetic model that best fits the experimental data. As such, the highest value of R^2 is conferred by the PFO model, as shown in Figure 4, suggests that the MB degradation process follows the PFO kinetic adsorption theory. This denotes that the adsorption rate of MB by the SAFE-AgNPs adheres through interfacial diffusion and that the maximum adsorption corresponds to a saturated monolayer of adsorbates on the adsorbent's surface (Khan and Thabaiti, 2022). Furthermore, the sorption only occurs on localized sites, and the spatial distribution of adsorbates is random, which means no spatial correlations exist between sites (Razdan and Bhan, 2021). The slope of the curve represents the rate constant, k, for the photodegradation of MB by the catalyst used (Farzi and Nezamzadeh-Ejhieh, 2022). These parameters were computed from the nonlinear graph derived from the model. Kinetic parameters obtained from the mathematical models used are shown in Table 1.

The previous report corroborated the results obtained in this study, where MB degraded and followed pseudo first order kinetics under sunlight irradiation over 6 hours of incubation with a 30-minute interval (Mechouche *et al.*, 2022).

To determine the photodegradation rate of MB, Langmuir-Hinshelwood (L-H) kinetic model was used and is described by the Equation (6).

$$v = \left(\frac{dMB}{dt}\right) = k_r\theta = k_r\frac{KMB}{1+KMB} \quad (6)$$

For very low concentrations $K<<1$, the equation becomes Equation (7).

$$-\ln\left(\frac{MB}{MB_0}\right) = k_{obs}t \quad (7)$$

k_r is the maximum photocatalytic reaction rate, K, is the adsorption coefficient of the reactant on the photocatalytic surface, MB is

the reactant concentration and k_{obs} is the observed first order rate constant. Equation (2) describes the rate of the photochemical reactions proportional to the surface coverage of the photocatalyst.

To establish the catalytic behavior of normalized concentration (ln MB/MBo) and reaction time of the samples, namely SAFE-AgNPs, synthetic AgNPs, and control, nonlinear relationships among them were derived applying L-H kinetic model. Two different light sources were used to ascertain the samples' catalytic properties. Based on the results, the model obeys pseudo-first-order kinetics as illustrated in Figure 4.

The regression line of ln MB/MBo as a function of time demonstrated a decrease in trend corroborating MB degradation, where MBo and MB refer to the initial and final concentrations of MB at a certain time, t, respectively. This result confirmed the assumption of L-H theory that the catalytic reactions of surface species towards the adsorbates are randomly distributed and that the rate of the MB photodegradation reaction is controlled by the species present in the monolayer of the surface interface (Sun *et al.*, 2023). These results complemented Lagergen's PFO adsorption kinetic model performed in this study. Similar findings were obtained by the study on the evaluation of the photocatalysis kinetics towards MB in an aqueous solution using a coupled cobalt (II) oxide-silver tungstate nano photocatalyst where the reaction followed PFO kinetics applying the L-H model (Sun *et al.*, 2023). Other findings showed consistent results with the dynamic behavior of the adsorption of MB on the activated charcoal coated monolith aqueous solutions where its kinetics followed the PFO kinetic adsorption model (Darmadi *et al.*, 2023).

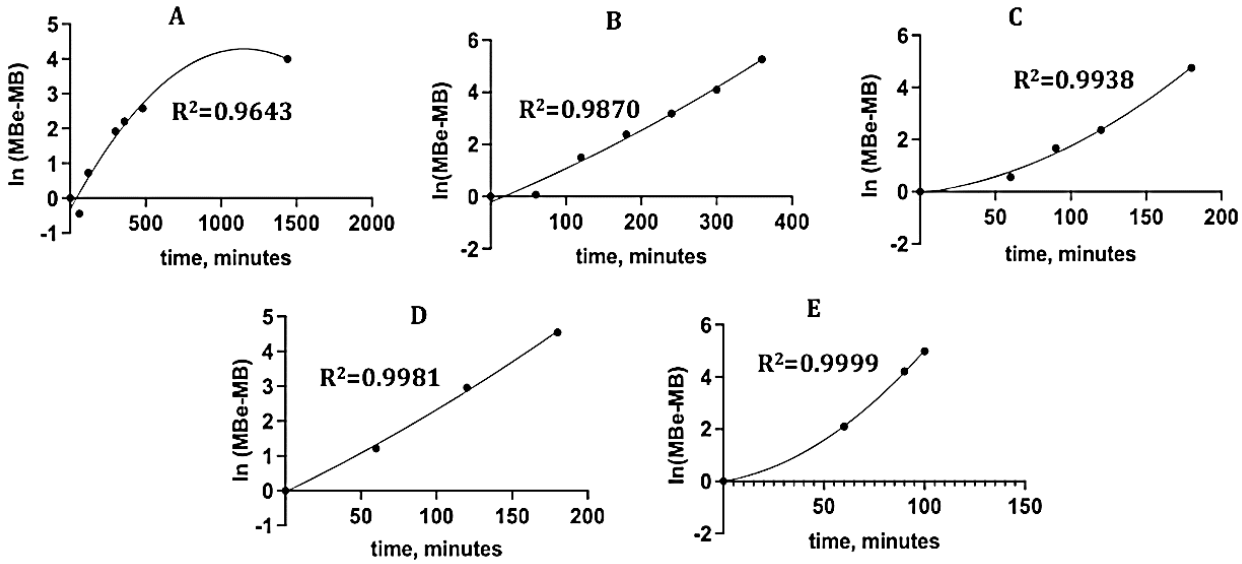

Fig. 4: The PFO kinetic plots of SAFE-AgNPs/AgNPs mediated photocatalytic degradation of MB dye. A) MB control; B) MB with AgNP (LED); C) MB with SAFE-AgNP (LED); D) MB with AgNP (SOLAR); E) MB with SAFE-AgNP (SOLAR).

DOI: 10.22146/ajche.82506

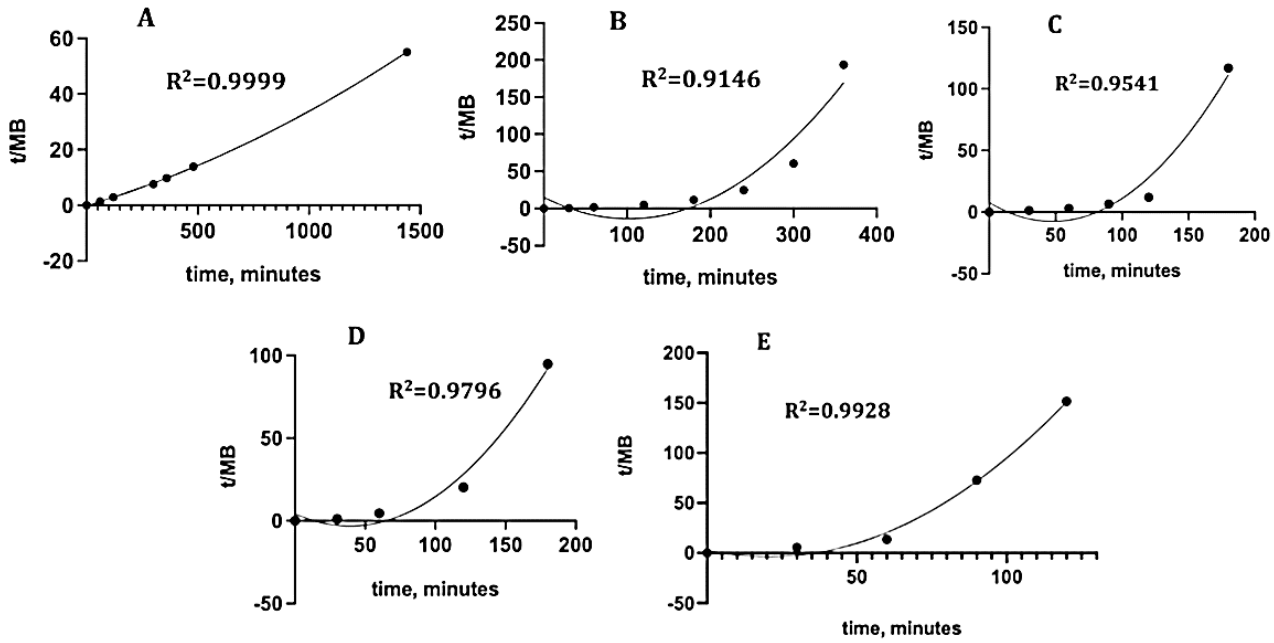

Fig. 5: The PSO kinetic plots of SAFE-AgNPs/AgNPs mediated photocatalytic degradation of MB dye. A) MB control; B) MB with AgNPs (LED); C) MB with SAFE-AgNPs (LED); D) MB with AgNPs (SOLAR); E) MB with SAFE-AgNPs (SOLAR).

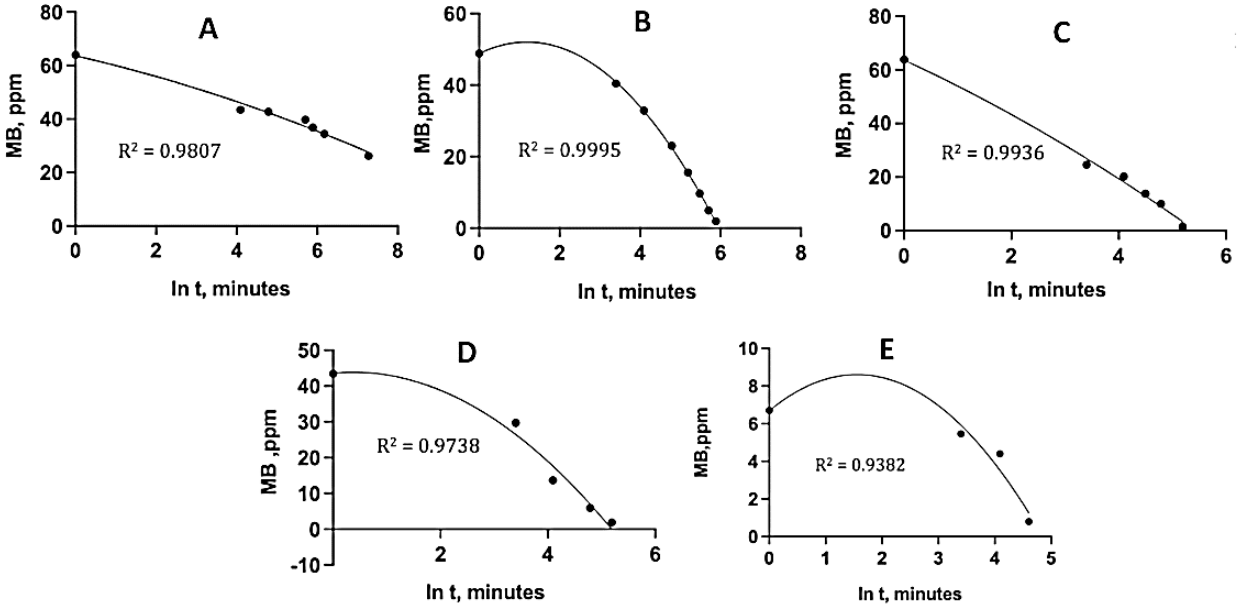

Fig. 6: The Elovich kinetic plots of SAFE-AgNPs/AgNPs mediated photocatalytic degradation of MB dye. A) MB control; B) MB with AgNPs (LED); C) MB with SAFE-AgNPs (LED); D) MB with AgNPs (SOLAR); E) MB with SAFE-AgNPs (SOLAR).

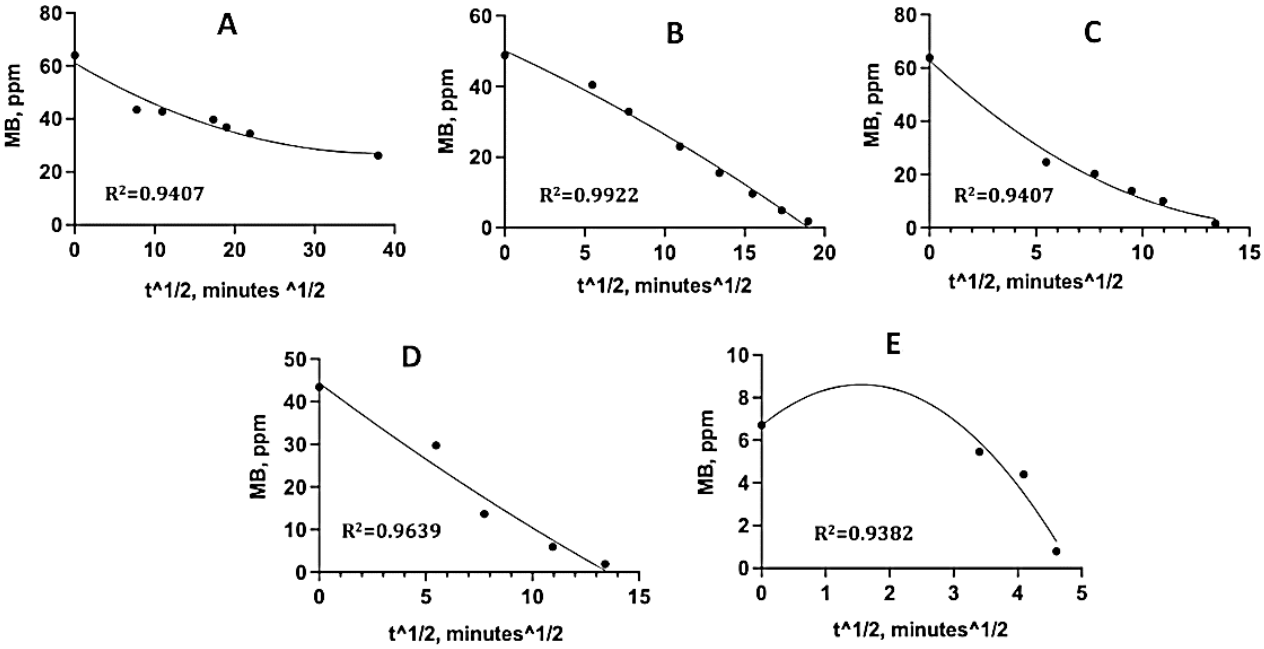

Fig. 7: The Intraparticle diffusion kinetic plots of SAFE-AgNPs/AgNPs mediated photocatalytic degradation of MB dye. A) MB control; B) MB with AgNPs (LED); C) MB with SAFE-AgNPs (LED); D) MB with AgNPs (SOLAR); E) MB with SAFE-AgNPs (SOLAR).

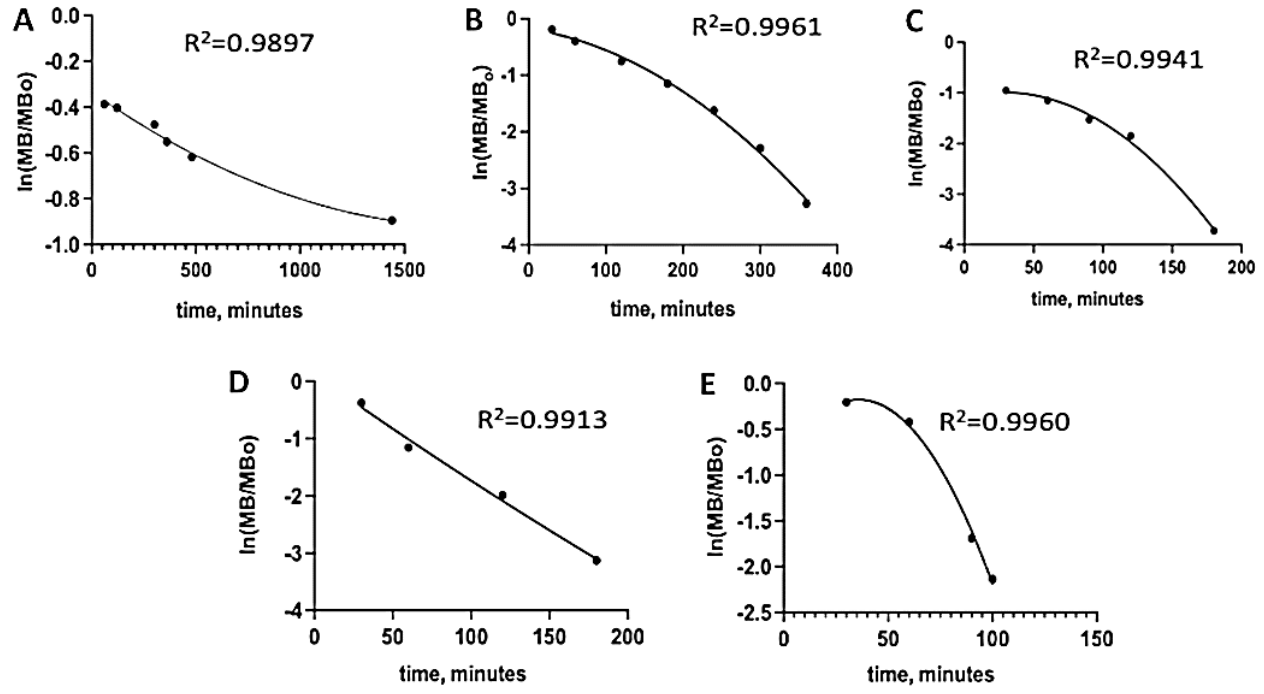

Fig. 8: Langmuir-Hinshelwood plots of SAFE-AgNPs/AgNPs mediated photocatalytic degradation of MB dye. A) MB control; B) MB with AgNPs (LED); C) MB with SAFE-AgNPs (LED); D) MB with AgNPs (SOLAR); E) MB with SAFE-AgNPs (SOLAR).

DOI: 10.22146/ajche.82506

Table 1. Kinetic parameters calculated from PFO, PSO, the Elovich, and the intraparticle diffusion models.

Sample/Catalyst	Light used	Kinetic Model used	R^2
Control	LED/sunlight	PFO	0.9643
SAFE-AgNPs	sunlight	PFO	0.9999
SAFE-AgNPs	LED	PFO	0.9938
Synthetic AgNPs	sunlight	PFO	0.9981
Synthetic AgNPs	LED	PFO	0.9870
Control	LED/sunlight	PSO	0.9999
SAFE-AgNPs	sunlight	PSO	0.9928
SAFE-AgNPs	LED	PSO	0.9541
Synthetic AgNPs	sunlight	PSO	0.9796
Synthetic AgNPs	LED	PSO	0.9146
Control	LED/sunlight	Elovich	0.9805
SAFE-AgNPs	sunlight	Elovich	0.9382
SAFE-AgNPs	LED	Elovich	0.9936
Synthetic AgNPs	sunlight	Elovich	0.9738
Synthetic AgNPs	LED	Elovich	0.9995
Control	LED/sunlight	IPD	0.9407
SAFE-AgNPs	sunlight	IPD	0.9382
SAFE-AgNPs	LED	IPD	0.9876
Synthetic AgNPs	sunlight	IPD	0.9639
Synthetic AgNPs	LED	IPD	0.9922
Control	LED/sunlight	LH	0.9897
SAFE-AgNPs	sunlight	LH	0.9960
SAFE-AgNPs	LED	LH	0.9941
Synthetic AgNPs	sunlight	LH	0.9913
Synthetic AgNPs	LED	LH	0.9961

Recyclability of SAFE-AgNPs

The photocatalytic efficiency of SAFE-AgNPs upon MB dye degradation was investigated. The catalyst was recovered after the complete degradation of the MB dye and was washed twice with DDI water to remove unwanted contamination from the previous analysis. After several runs, the reusability data of SAFE-AgNPs displayed high efficacy due to minimal activity loss, as shown in Figure 9A. This indicates a favorable catalytic property of SAFE-AgNPs. Furthermore, the absorbance spectrum of the recovered catalyst, SAFE-AgNPs, remained the same at 415 nm, indicating no further oxidation occurred during the several degradation runs, as shown in Figure 9B. Similar findings were observed in the catalytic performance of the r-GO AgNPs, where a slight reduction was observed during the reaction process (Khan *et al.*, 2020).

As evinced by the efficient photo-degradation potential of SAFE-AgNPs, a possible general mechanism is proposed. See Figure 10. When the light strikes the electrons of SAFE-AgNPs, it causes excitation of these electrons from the valence to the conduction band of SAFE-AgNPs generating positive electron hole pairs (hν+). The positive electron hole pairs react with the hydroxide

ion and water, forming the hydroxyl radicals. In contrast, the photogenerated electrons react with the environment's molecular oxygen to form the superoxide radical. The highly energetic free radicals then react with MB to reduce it to leucomethylene blue, finally broken down into nontoxic fragments like CO_2 and H_2O (Konstantinou and Albanis, 2004). These free radicals are believed to be the cause of the degradation of MB dye. On the other hand, those substrates unreactive with the free radicals were degraded and hypothesized to be associated with the catalytic properties of SAFE-AgNPs (Tanaka *et al.*, 2000).

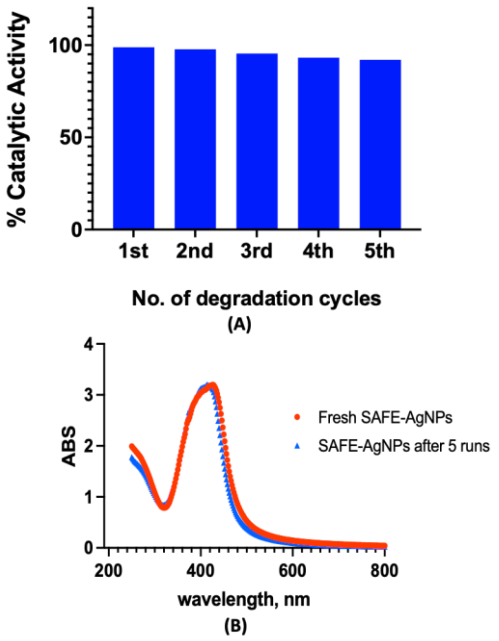

Fig. 9: Catalytic activity of SAFE-AgNPs. A) Reusability tests of SAFE-AgNPs in MB degradation.; B) UV-Vis absorption spectra before and after 5 degradation cycles.

CONCLUSION

The small, spherical, and stable properties of SAFE-AgNPs have a high surface-to-volume ratio, which exhibited a promising photocatalytic property to degrade MB. As such, 98.8 % (SOLAR) and 97.6% (LED) degradation rates of MB photodegradation were achieved. The photocatalytic kinetics fit the Langmuir-Hinshelwood pseudo first order model with an R2 value of 0.9960 and 9.9941 under sunlight and LED light irradiations, respectively. This denotes that the catalytic reactions of SAFE-AgNPs towards the adsorbates are randomly distributed and that the rate of the MB photodegradation reaction is controlled by the species present in the monolayer of the surface interface. These results complemented Lagergen's PFO adsorption kinetic model performed in the study. The developed green process can be an alternative approach to conventional methods in synthesizing biogenic silver nanoparticles, which may be useful for photocatalytic environmental remediation.

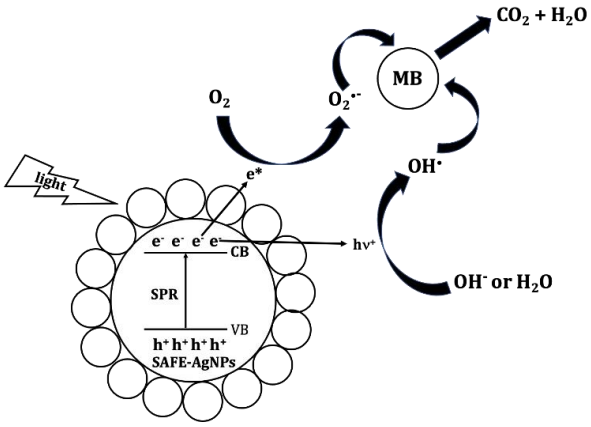

Fig. 10: The schematic diagram of the proposed molecular mechanism of the photodegradation of MB dye using SAFE-AgNPs. When sunlight or LED light strikes the MB solution with SAFE-AgNPs, electrons get excited, generating positive electron hole pairs. The generated electron hole pairs react with the hydroxide ion to form free radicals. These radicals degrade the MB dye forming nontoxic products like CO_2 and H_2O.

DOI: 10.22146/ajche.82506

It is recommended that future researchers design a reactor in a large-scale setting to produce a sufficient amount of AgNPs for photocatalytic experiments that could be used for the treatment of industrial wastewater.

REFERENCES

Abbasi, E., Milani, M., Aval, S.F., Kouhi, M., Akbarzadeh, A., Nasrabadi, H.T., Nikasa, P., Joo, S.W., Hanifehpour, Y., Nejati-Koshki, K., and Samiei, M., 2016. "Silver nanoparticles: Synthesis methods, bio-applications and properties." *Critical Review Microbiology 42(2),* 173–180.

Ajay, S., Panicker, J.S., Manjumol, K.A., and Subramanian, P.P., 2022. "Photocatalytic activity of biogenic silver nanoparticles synthesized using *Coleus Vettiveroids*." *Inorganic Chemistry Communications 144,* 109926

Aurich A., Hofmann J., Oltrogge R., Wecks M., Gläser R., Blömer L., et al., 2017. "Improved isolation of microbiologically produced (2R,3S)-isocitric acid by adsorption on activated carbon and recovery with methanol." *Org. Process Res. Dev. 21(6),* 866–870.

Banerjee K., 2012. "A novel agricultural waste adsorbent, watermelon shell for the removal of copper from aqueous solutions." *Iran. J. Energy Environ. 3(2),* 143-156.

Chen, C.C., Lu, C.S., Chung, Y.C., Jan, J.L., 2007. "UV light induced photodegradation of malachite green on TiO_2 nanoparticles." *Journal of Hazardous Materials 141(3),* 520–528.

Darmadi D., Choong, T.S.Y., Chuah, T.G, Yunus R., Taufiq Yap, Y.H., 2008. "Adsorption of methylene blue from aqueous solutions on carbon coated monolith." *ASEAN Journal of Chemical Engineering 8 (1),* 26–37.

Edison, T.J.I., and Sethuraman, M.G., 2012. "Instant green synthesis of silver nanoparticles using Terminalia chebula fruit extract and evaluation of their catalytic activity on reduction of methylene blue." *Process Biochemistry 47(9),*1351–1357.

Fahimirad, S., and Hatami, M., 2017. "Heavy metal-mediated changes in growth and phytochemicals of edible and medicinal plants in *Medicinal Plants and Environmental Challenges,* Springer, Cham, Germany, pp.189–214.

Farsi, M., and Nezamzadeh-Ejhieh, A., 2022. "A coupled cobalt (II) oxide-silver tungstate nano-photocatalyst: Moderate characterization and evaluation of the photocatalysis kinetics towards methylene blue in aqueous solution." *Polyhedron 219*, 115823.

Ghorbanpour, M., and Fahimirad, S., 2017. "Plant nanobionics a novel approach to overcome the environmental challenges in Medicinal Plants and Environmental Challenges, Springer, Cham, Germany, pp. 247–257.

Gowda S.A.M, Goveas L.C, Dakshayini K., 2022. "Adsorption of methylene blue by silver nanoparticles synthesized from Urena lobata leaf extract: Kinetics and equilibrium analysis." *Mater. Chem. Phys. 288*, 126431.

Gupta, N., Singh, H.P., and Sharma, R.K., 2011. "Metal nanoparticles with high catalytic activity in degradation of methyl orange: An electron relay effect." *Journal of Molecular Catalysis A: Chemical 335 (1–2)*, 248–2452.

Ho, Y.S., 2006. "Review of second-order models for adsorption systems." *J. Hazard Mater. 136(3),* 681–689.

Ho, Y., and McKay, G., 2000. "The kinetics of sorption of divalent metal ions onto sphagnum moss peat." *Water Res. 34(3)*, 735-742.

Ji, X., Kan, G., Jiang, X., Sun, B., Zhu, M., and Sun, Y., 2018. "A monodisperse anionic silver nanoparticles colloid: Its selective adsorption and excellent plasmon-induced photodegradation of methylene blue." *Journal of Colloid Interface Science 523*, 98–109.

Khan, Z., and AL-Thabaiti, S.A., 2022. "Chitosan capped silver nanoparticles: Adsorption and photochemical activities." *Arabian Journal of Chemistry 15(11),*104154.

Khan, Z.U.H., Shah, N.S., Iqbal, J., Khan, A.U., Imran, M., Alshehri, S.M., Muhammad, N., Sayed, M., Ahmad, N., Kousar, A., Ashfaq, M., Howari, F.M., & Tahir, K., 2013. "Biomedical and photocatalytic applications of biosynthesized silver nanoparticles: Ecotoxicology study of brilliant green dye and its mechanistic degradation pathways." *Journal of Molecular Liquids 319*, 114114.

Kharissova, O.V., Dias, H.V.R., Kharisov, B.I., Pérez, B.O., and Pérez, V.M.J., 2013. "The greener synthesis of nanoparticles." *Trends in Biotechnology 31(4),*240–8.

Konstantinou, I.K., and Albanis, T.A., 2004. "TiO_2-assisted photocatalytic degradation of azo dyes in aqueous solution: Kinetic and mechanistic investigations: A review." *Applied Catalysis B: Environmental 49*, 1–14.

Kumar, B., Vizuete, K.S., Sharma, V., Debut, A., and Cumbal, L., 2019. "Ecofriendly synthesis of monodispersed silver nanoparticles using Andean Mortiño berry as reductant and its photocatalytic activity." *Vacuum 160*, 272–278.

Martin, M.M., and Sumayao, Jr. R.E., 2022. "Facile green synthesis of silver nanoparticles using *Rubus rosifolius Linn* aqueous fruit extracts and its characterization." *Applied Science in Engineering Progress 15(3),* 5511.

Mehwish, H.M., Rajoka, M.S.R., Xiong, Y., Cai, H., Aadil, R.M., Mahmood Q, He, Z., and Zhu, O., 2021. "Green synthesis of a silver nanoparticle using *Moringa oleifera* seed and its applications for antimicrobial and sun-light mediated photocatalytic water detoxification." *Journal of Environmental Chemical Engineering 9(4)*, 105290.

Mechouche, M.S., Merouane, F., Messaad C.E.H., Golzadeh, N., Vasseghian. Y., and Berkani, M., 2022. "Biosynthesis, characterization, and evaluation of antibacterial and photocatalytic methylene blue dye degradation activities of silver nanoparticles from *Streptomyces tuirus strain*." *Environmental Research 1*, 204

Razdan, N.K., and Bhan, A., 2021. "Catalytic site ensembles: A context to reexamine the Langmuir-Hinshelwood kinetic description." *Journal of Catalysis 404*, 726–44.

Rostami-Vartooni, A., Nasrollahzadeh, M., Salavati-Niasari, M., and Atarod, M., 2016. "Photocatalytic degradation of azo dyes by titanium dioxide supported silver nanoparticles prepared by a green method using *Carpobrotus acinaciformis* extract." *Journal of Alloys and Compounds 689*,15–20.

Ruíz-Baltazar Á. de J., 2020. "Kinetic adsorption models of silver nanoparticles biosynthesized by Cnicus Benedictus: Study of the photocatalytic degradation of methylene blue and antibacterial activity." *Inorg. Chem. Commun. 120*, 108158.

DOI: 10.22146/ajche.82506

Saha, D., and Grappe, H.A., 2017. "Adsorption properties of activated carbon fibers." *Activated Carbon Fiber and Textiles 1*, 43–65.

Singh, J., and Dhaliwal, A.S., 2020. "Plasmon-induced photocatalytic degradation of methylene blue dye using biosynthesized silver nanoparticles as photocatalyst." *Environmental Technology 41(12)*,1520–1534.

Sioson A.C, Gallardo S.M., 2008. "Photodegradation of chlordane in soil and water matrix using induced uv and solar light." *ASEAN Journal of Chemical Engineering 7 (1-2),* 30–42.

Sun, W., Hong, Y., Li, T., Chu, H., Liu, J., Feng, L., and Baghaveri, M., 2023. "Biogenic synthesis of reduced graphene oxide decorated with silver nanoparticles (rGO/Ag NPs) using table olive (olea europaea) for efficient and rapid catalytic reduction of organic pollutants." *Chemisphere 310*,136759.

Tanaka, K., Padermpole, K., and Hisanaga, T., 2000. "Photocatalytic degradation of commercial azo dyes." *Water Research 34*, 327–333.

Varadavenkatesan, T., Selvaraj, R., and Vinayagam, R., 2016. "Phyto-synthesis of silver nanoparticles from Mussaenda erythrophylla leaf extract and their application in catalytic degradation of methyl orange dye." *Journal of Molecular Liquids 221*,1063–1070.

Venkateswarlu P, Ratnam MV, Rao DS, Venkateswara Rao M., 2007. "Removal of chromium from an aqueous solution using *Azadirachta indica (neem)* leaf powder as an adsorbent." *Int. J. Phys. Sci. 2 (8),* 188-195.

WEPA, 2015, Water Environment Partnership in Asia, http://wepa-.net/policies/state/philippines/overview.html.